13

Magnetic field visualization in scanning electron microscope

© D.A. Tatarskiy,[1,2] E.V. Skorokhodov,[1] S.A. Gusev[1]

[1] Institute for Physics of Microstructures RAS,
603087 Afonino village, Kstovsky district, Nizhny Novgorod region, Russia
[2] Lobachevsky University of Nizhny Novgorod,
603950 Nizhny Novgorod, Russia
e-mail: tatarsky@ipmras.ru

Received April 12, 2023
Revised April 12, 2023
Accepted April 12, 2023

The fundamental possibility of measuring the stray fields distributions of magnetic objects in a scanning electron microscope is demonstrated. The main idea of the method is to use a sample holder for operation in the mode of a scanning transmission microscope, additionally equipped with a square diffraction grating. This grating, formed on the basis of a metal film, is placed at some distance under the magnetic sample. Reconstruction of the deflections of transmitted electrons by analyzing the geometric phase from visible distortions of the diffraction grating made it possible to reconstruct the distribution of the magnetic field created by the sample under study.

Keywords: magnetic field, scanning electron microscope, lorentz microscopy, magnetic nanostructures.

DOI: 10.61011/TP.2023.07.56643.81-23

Introduction

There are several microscopic methods for obtaining images of magnetization and stray fields created by nano- and micro-objects. The most informative method of quantitative measurements of magnetic states is electron holography, used in the study of nanostructures using transmission electron microscopy. The method is based on the fact that initially a electron plane wave acquires a different phase along its front when passing through a magnetized sample or an inhomogeneous magnetic field due to the Aharonov–Bohm effect [1,2]. At the same time, two main methods are divided: off-axis holography [3] and axial (inline) holography [4]. In the first method the phase of the wave function of the electrons passing through the sample is determined by an interferogram with a reference coherent plane wave. In the second method the phase is calculated by solving the inverse problem using the transfer-of-intensity equation using focal series of microphotographs. The disadvantages of off-axis holography include the need for additional equipment of a transmission electron microscope with an electrostatic biprism and a small field of view (up to several μm^2). Axial holography is devoid of such disadvantages, but requires the use of advanced mathematical methods and taking into account the distortion of microphotographs depending on the degree of defocusing [5]. Holographic methods of electron microscopy have the best spatial resolution, but the complexity of their implementation often forces the use of simpler methods of Lorentz microscopy.

A new modification of the Lorentz microscopy method has recently been proposed, which can be implemented in any scanning electron or ion microscope [6]. The idea of the method is to use a sample holder in a conventional scanning microscope, which allows images to be recorded in a transmission mode, and is additionally equipped with a diffraction grating located below the sample. In this case, the visualization of electromagnetic fields consists in measuring electron deviations by registering distortions of the diffraction grating image. Note that this is not the only option for measuring magnetic fields in SEM. Thus, fitting the SEM with a multi-section detector allows measuring the distribution of magnetic fields by the method of differential phase contrast [7] in the transmission mode of operation. The addition of the SEM with the Mott detector, which registers the spin polarization of secondary electrons, makes it possible to study the magnetization of the surface of magnetic materials by scanning electron microscopy with polarization analysis (SEMPA) [8,9]. The disadvantages of both methods include the need to equip a serial SEM with an appropriate type of expensive detector, in addition, the SEMPA method sets requirements for the quality of the vacuum in the microscope chamber during measurements [10]. It should also be noted that there is a method of magnetic force microscopy, which, like the SEMPA method, allows estimating the magnetization distributions in thin ferromagnetic films [11]. At the same time, the method of magnetic force microscopy, provides only qualitative information about the stray fields above the sample, while quantitative measurements require additional time-consuming calibrations of each used probe of the magnetic force microscope pa [12–14].

This paper demonstrates the possibility of determining the configuration of the magnetic field around a magnetized needle using the method of raster electronic mapping. As will be shown, this method is not only easily implemented on any serial SEM, but also provides quantitative information about the distribution of magnetic fields.

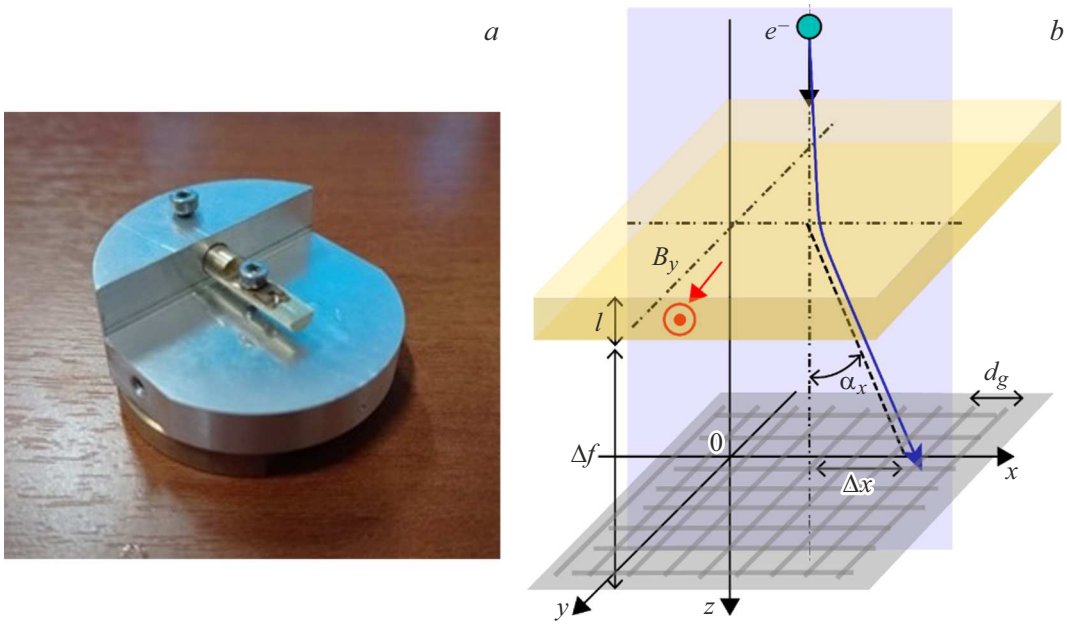

Figure 1. *a* — sample holder for scanning electron microscope, which allows working with the sample „in the transmission mode“; *b* — schematic representation of the change in the trajectory of electrons under the impact of the Lorentz force in a magnetic field.

1. Samples and methods

Supra 50 VP scanning electron microscope (Carl Zeiss, Jena) for which a sample holder was made was used in this paper (Fig. 1, *a*). A diffraction grating with square cells and a period of 6 μm was located under the sample at some distance on the flat surface of the holder. The width of the grating bar was 3 μm. The diffraction grating was made of a gold film with a thickness of 30 nm on a silicon substrate by laser optical lithography using a laser microimage generator mPG101.

During the passage of an electron beam in an inhomogeneous magnetic field created by the sample, under the influence of the Lorentz force, their deviation from the linear trajectory occurs, resulting in distortion in the image of the diffraction grating (Fig. 1, *b*). These images were recorded using the Everhart–Thornley secondary electron detector. A sufficient depth of focus is the main requirement for observing distortions in the diffraction grating image. It is necessary that the depth of focus be comparable to the distance from the object to the diffraction grating. In this case, both in the region of the stray field of the sample and in the region of the diffraction grating, the electron beam remains collimated. The smallest 10 μm aperture and a large working distance (12–20 mm) were used to fulfill this condition in the experiment.

The visible distortion of the diffraction grating was estimated by the geometric phase analysis method [15,16]. Mathematically, this method consists in the fact that the distortions of the diffraction grating are calculated from the peak of the Fourier image of the original image. The phase in this case is the difference between the grating and the ideal periodic structure.

Suppose that the Lorentz force acts on an electron from the side of a homogeneous magnetic field localized in a layer with a thickness of l (Fig. 1, *b*). The deflection angle α is easy to estimate

$$\alpha = \frac{e}{h} B_{\parallel} l \lambda,$$

where e is the electron charge, h is the Planck constant, λ is the length electron waves, $B_{\parallel}$ is the magnitude of magnetic induction. The magnetic induction is determined using this formula, and the angle α is estimated based on the distortion of the diffraction grating

$$B_{\parallel}(x, y) = \frac{h}{e} \frac{1}{l\lambda} \frac{d_g}{\Delta f} \frac{\varphi(x, y)}{2\pi},$$

where d_g is the step of the diffraction grating, Δf is the amount of defocusing, which here is equal to the distance between the sample and the diffraction grating. It is easy to estimate the magnitude of the magnetic field flux between adjacent lines of constant phase $\varphi(x, y) = \text{const}$. It is enough to multiply $B_{\parallel}(x, y)$ by „elementary“ area $d_g l$:

$$\Phi = \frac{d_g^2}{\lambda \Delta f} \Phi_0,$$

where $\Phi_0 = h/e$ is the quantum of magnetic flux. Two samples such as two uniformly magnetized needles made of ferromagnetic material were prepared for experiments. The measurements were carried out at various accelerating voltages.

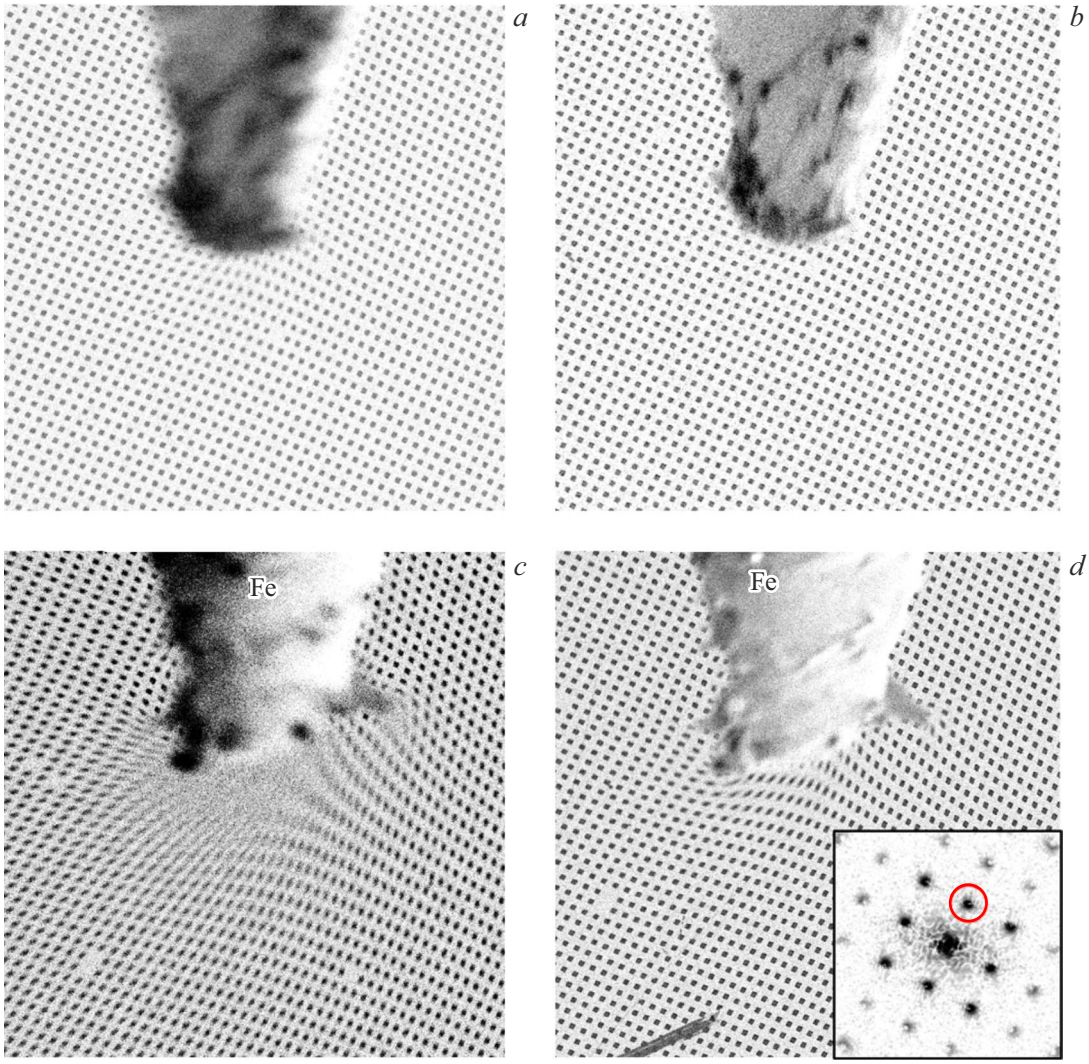

Figure 2. Distortion of the diffraction grating around ferromagnetic needles (a, b). A needle with a small magnetic moment at accelerating voltages of 2 and 10 kV (c, d). A needle with a large magnetic moment at accelerating voltages of 2 and 10 kV. The size of each frame is $250 \times 250\,\mu$m. The insert shows an example of a Fourier image of an image and marks the reflex used for phase reconstruction.

2. Results and discussion

Figure 2 shows micrographs of a diffraction grating in secondary electrons during the passage of a primary electron beam in the vicinity of two ferromagnetic needles with small and large magnetic moments. Micrographs were acquired at two values of the accelerating voltage — 2 and 10 kV.

The amount of defocusing was determined by the difference between the two working distances of the SEM, when, when receiving images, accurate focusing was carried out either on the tip of the needle or on the diffraction grating. For both needles, this value was $\Delta f = 1.2$ mm, which gives the following flow values $\Phi = 1094\Phi_0$ and $2439\Phi_0$ with a phase difference 2π for accelerating voltages 2 and 10 kV, respectively. Reconstruction of the spatial distribution of the phase of image distortion was carried out in the Gatan Microscopy Suite 3.5.0 software package using a special script [17]. In all cases, Fourier peaks (010) were used to analyze the geometric phase (insert in Fig. 2). The reconstruction results are shown in Fig. 3.

The density of lines with a phase difference should increase approximately by $2439/1094 \approx 2.2$ times with a decrease of the accelerating voltage. It is easy to see that there is such a correspondence between the pairs of Fig. 3, *a, b* and *c, d*. The density of the constant phase lines can also be used to estimate the difference in magnetic moments between the two needles. The ratio of magnetic moments of samples with low and high magnetization is approximately from 3 to 4 in our experiment.

The registration of units of magnetic flux quanta [18–20] is required to measure the magnetic stray fields of the tip of a magnetic force probe or, for example, magnetic skyrmions or vortices in patterned nanostructures. It is easy to estimate that if the diffraction grating period is reduced by a factor of 10, this will give $\Phi = 11\Phi_0$ for an accelerating voltage of 2 kV, and will allow quantitative measurements of magnetic

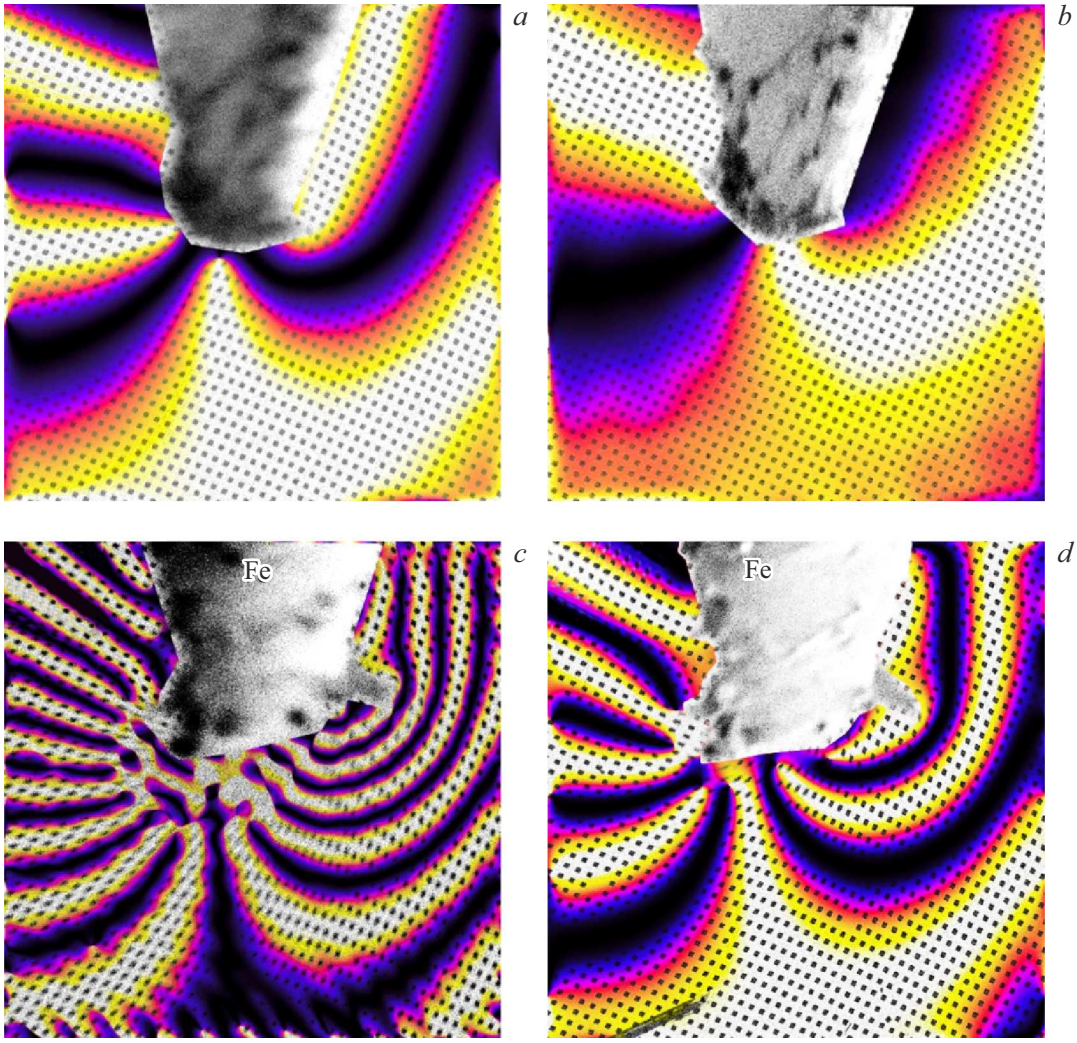

Figure 3. Phase distribution of the diffraction grating distortions superimposed on the original microphotography. *a, b* is a sample with a small magnetic moment at accelerating voltages 2 and 10 kV; *c, d* — a sample with a large magnetic moment at accelerating voltages 2 and 10 kV. The size of each frame is $250 \times 250\,\mu$m.

fields in nanostructures. In addition, if we consider the magnetization distributions in patterned nanostructures that do not have stray fields, it becomes possible to measure the magnitude of magnetization. For example, the magnetostatic field of a magnetic vortex in a thin disk is localized near its core (center). Therefore, we will actually carry out magnetization measurements by estimating the electron deflection closer to the edge of the disk using this method. Indeed, in this case, the thickness of the layer in which the magnetic field is localized coincides with the thickness of the magnetic film and it is possible to derive the magnitude of magnetic induction and magnetization directly from the magnetic field flux.

Conclusions

The paper demonstrates the fundamental possibility of reconstruction of the spatial distribution of magnetic stray fields in ferromagnetic samples using a standard scanning electron microscope without buying additional expensive equipment, for example, a multisectoral detector of transmitted electrons. These measurements are based on the analysis of image distortions of the periodic lattice, which are caused by deviations of electron beams under the action of the Lorentz force. It is shown that in such experiments it is possible to measure fields up to tens of magnetic flux quanta. Note that this method provides quantitative estimates of the magnetic field and can be used not only to visualize the distribution of the magnetic field, but also to determine the magnetization values of thin films and nanostructures. Since electron beams can change their trajectories in electric fields, a similar technique is also applicable for the diagnosis of these fields created by electric charges, which was demonstrated in the work [6]. Thus, the described method can be used as a full-fledged replacement for expensive standard holographic electron microscopy methods.

Acknowledgments

The authors thank I.Y. Pashenkin and D.V. Bratanich for useful discussions. The equipment of the Centre for Collective Use „Physics and Technology of Micro- and Nanostructures“ equipment was used in the study (Institute for Physics of Microstructures of Russian Academy of Sciences).

Funding

This paper was supported by grant of the Russian Science Foundation № 21-72-10176.

Conflict of interest

The authors declare that they have no conflict of interest.

References

[1] Y. Aharonov, D. Bohm. Phys. Rev. B, **115**, 485 (1959).
[2] A. Tonomura, N. Osakabe, T. Matsuda, T. Kawasaki, J. Endo, S. Yano, H. Yamada. Phys. Rev. Lett., **56**, 792 (1986).
[3] T. Tanigaki, K. Harada, Y. Murakami, K. Niitsu, T. Akashi, Y. Takahashi, A. Sugawara, D. Shindo. J. Phys. D: Appl. Phys., **49**, 244001 (2016).
[4] A. Kohn, A. Habibi, M. Mayo. Ultramicroscopy, **160**, 44 (2016).
[5] M. Huang, A. Eljarrat, C. Koch. Ultramicroscopy, **231**, 113264 (2021).
[6] K. Harada, K. Shimada, Y. Takashi. Microscopy, **71**, 93 (2022).
[7] J.N. Chapman, I.R. McFadyen, S. McVitie. IEEE Transactions on Magnetics, **26**, 1506 (1990).
[8] M.R. Scheinfein, J. Unguris, M.H. Kelley, D.T. Pierce, R.J. Celotta. Rev. Scientific Instruments, **61**, 2501 (1990).
[9] T. Kohashi, K. Koike. Jpn. J. Appl. Phys., **40**, L1264 (2001).
[10] S.A. Gusev, V.N. Petrov, E.V. Skorokhodov. Poverkhnost. Rentgenovskie, sinkhrotronnye i neitronnye issledovaniya, *7*, 40 (2010) (in Russian).
[11] V.L. Mironov. *Osnovy skaniruyushchei zondovoi mikroskopii* (IFM RAN, Nizhnii Novgorod, 2004) (in Russian)
[12] L. Kong, St.Y. Chou, J. Appl. Phys., **81**, 5026 (1997).
[13] P.J.A. van Schendel, H.J. Hug, B. Stiefel, S. Martin, H.-J. Güntherodt. J. Appl. Phys., **88**, 435 (2000).
[14] D. Nečas, P. Klapetek, V. Neu, M. Havlıček, R. Puttock, O. Kazakova, X. Hu, L. Zajíčková. Scientific Reports, **9**, 3880 (2019).
[15] M.J. Hÿtch, E. Snoeck, R. Kilaas. Ultramicroscopy, **74**, 131 (1998).
[16] J.L. Rouvière, E. Sarigiannidou. Ultramicroscopy, **106**, 1 (2005).
[17] K.-H. Kim. Appl. Micro., **45**, 101 (2015).
[18] V. Panchal, H. Corte-León, B. Gribkov, L.A. Rodriguez, E. Snoeck, A. Manzin, E. Simonetto, S. Vock, V. Neu, O. Kazakova, Scientific Reports, **7**, 7224 (2017).
[19] V. Boureau, M. Stano, J.-L. Rouviere, J.-Ch. Toussaint, O. Fruchart, D. Cooper. J. Phys. D: Appl. Phys., **54**, 085001 (2021).
[20] H.S. Park, X. Yu, Sh. Aizawa, T. Tanigaki, T. Akashi, Y. Takahashi, T. Matsuda, N. Kanazawa, Y. Onose, D. Shindo, A. Tonomura, Y. Tokura. Nature Nanotech., **9**, 337 (2014).

Translated by A.Akhtyamov